



Differences in the temporal expression of regulatory growth factors during choroidal neovascular development

Wenzheng Hu^{a,b}, Mark H. Criswell^{a,b,*}, Shao-Ling Fong^a, Constance J. Temm^b, Gangaraju Rajashekhar^b, Tammy L. Cornell^a, Matthias A. Clauss^b

^a Department of Ophthalmology, Indiana University School of Medicine, 702 Rotary Circle, Indianapolis, IN 46202, USA

^b Indiana Center for Vascular Biology and Medicine, Indiana University School of Medicine, Indianapolis, IN 46202, USA

ARTICLE INFO

Article history:

Received 29 January 2008

Accepted in revised form 14 October 2008

Available online 1 November 2008

Keywords:

choroidal neovascularization
vascular endothelial growth factor
basic fibroblast growth factor
hepatocyte growth factor
laser photocoagulation
angiogenesis
anastomoses
neovascular hyperpermeability

ABSTRACT

Although the roles of vascular endothelial growth factor (VEGF), basic fibroblast growth factor (bFGF), and hepatocyte growth factor (HGF) in pathologic neovascularization have been well characterized in certain tissues, their particular functions and expression patterns in choroidal neovascularization (CNV) have not been clearly established. After localized laser trauma to Bruch's membrane to induce CNV development, the temporal changes in mRNA and protein expression of these 3 cytokines were documented and compared histologically to areas of immunofluorescence, the proliferation of endothelial cells, neovascular development, and temporal changes in vascular permeability. Changes in mRNA and protein levels of bFGF and HGF occurred quickly and reached peak expression within hours. This activity corresponded in time to intense and localized immunofluorescence for these cytokines within the choriocapillaris within laser lesion sites. During this same initial time period, mRNA upregulation of VEGF occurred, primarily within the neural retina and this expression corresponded to intense immunolabeling of Müller cells immediately adjacent to the lesion sites. By 3 days after laser, increased VEGF₁₆₄ protein expression was measurable, whereas early neovascular development histologically corresponded to HGF and bFGF mRNA expansion into the developing choroidal neovascular membrane (CNVM). At 7 days, CNV expansion, maturation, and increased vascular permeability corresponded to peak VEGF mRNA and protein expression and to immunofluorescence of the CNVM. Differences also occurred in the expression of precursor and activated isoforms of these cytokines in the retinal pigment epithelium/choroid as compared to those in the retina. These molecular and immunocytochemical results suggest that bFGF and HGF may be important as initial regulators neovascularization in this CNV model; whereas VEGF may be important during later phases of angiogenesis and neovascular hyperpermeability.

© 2008 Elsevier Ltd. All rights reserved.

1. Introduction

Choroidal neovascularization (CNV) is an important component of posterior segment diseases and results from complex interactions between angiogenic regulators that promote and/or inhibit endothelial cell differentiation, proliferation, and migration, as well as vascular maturation, stabilization, maintenance and permeability. Numerous angiogenic regulators participate in CNV development, including three multifunctional growth factors that possess the potential to affect multiple aspects of the angiogenic process: vascular endothelial growth factor (VEGF) (Frank et al.,

1996; Kvant et al., 1996; Spilsbury et al., 2000; Lip et al., 2001; Wang et al., 2003), basic fibroblast growth factor (bFGF or FGF-2) (Frank et al., 1996; Ogata et al., 1996), and hepatocyte growth factor (HGF or scatter factor) (Grierson et al., 2000).

VEGF functions as a potent mitogen in embryogenesis and in tumorigenesis, but its specific angiogenic roles in CNV have been largely based on inferential evidence. In age-related macular degeneration (AMD) patients, elevated VEGF expression has been demonstrated in patient vitreous samples and immunostained ocular tissues from preexisting neovascularization, although the exact relationship of VEGF to CNV angiogenesis remains under investigation. VEGF signaling also occurs after laser-induced rupture of Bruch's membrane evokes CNV (Kwak et al., 2000). Subretinal or vitreal infusion of exogenous VEGF can evoke experimental CNV, but then so can the over expression of other angiogenic regulators, including pigment epithelium derived factor (PEDF) which typically demonstrates antiangiogenic properties (Apte et al., 2004).

* Corresponding author. Department of Ophthalmology, Indiana University School of Medicine, 702 Rotary Circle, Indianapolis, IN 46202-5175, USA. Tel.: +1 317 274 2836; fax: +1 317 274 2838.

E-mail address: mcriswel@iupui.edu (M.H. Criswell).

VEGF upregulation can occur in endothelial cells of forming capillaries as a consequence of increased bFGF expression (Seghezzi et al., 1998; Shen et al., 1998; Wada et al., 1999). VEGF release from aging and damaged blood vessels may be one of the signaling molecules for circulating endothelial cells (CECs) and endothelial precursor cells (EPCs) during early postnatal vasculogenesis; however, bFGF is more potent than VEGF as a mitogenic activator for CEC proliferation (Zubilewicz et al., 2001; Wang et al., 2005). Nevertheless, bFGF is not considered able to singularly evoke CNV development (Tobe et al., 1998; Ishida et al., 1999; Campochiaro, 2000; Nagineni et al., 2003; Rosenthal et al., 2005; Hoffmann et al., 2006). While bFGF may be one of the initial inducers of endothelial cell proliferation, VEGF, in parallel or subsequently, is another mediator of this process.

HGF is a plasminogen-derived, multifunctional heterodimeric polypeptide produced by mesenchymal cells and it activates cells that express the Met tyrosine kinase receptor (Bottaro et al., 1991; Rubin et al., 1993). HGF can elicit mitogenic, motogenic, and morphogenic effects in various epithelial and endothelial cell types (Bussolino et al., 1992; Rubin et al., 1993; Nakamura et al., 1995; Matsumoto and Nakamura, 1996). HGF can mediate epithelial mesenchymal transition (Tsarfaty et al., 1994), the formation of vascular tubules and lumens (Montesano et al., 1991; Tsarfaty et al., 1992), and can independently and sufficiently induce and promote angiogenesis (Rosen et al., 1993a; Silvagno et al., 1995; Aoki et al., 2000; Taniyama et al., 2001a,b). HGF also can operate independently in mediating intraocular angiogenesis (Grierson et al., 2000). HGF signaling for retinal microvascular endothelial cell growth and migration is through the activation of PKC and phosphatidylinositol-3-kinase (PI3K) pathways, inducing MAPK phosphorylation (Cai et al., 2000). VEGF also can activate PKC, MAPK, and PI3K pathways (Xia et al., 1996). Although MAPK phosphorylation and mitogenesis can be blocked by an anti-VEGF antibody, HGF-induced MAPK phosphorylation and early HGF-induced mitogenesis neither require nor are affected by VEGF (Sengupta, S., et al., 2003). Therefore, HGF and VEGF are considered to operate in parallel and may possibly evoke synergistic actions during angiogenesis, although under certain circumstances HGF also may function as a VEGF inhibitor (Gerritsen, 2005).

Although the roles of VEGF, bFGF, and HGF in developmental, normal physiologic and pathologic neovascularization have been well characterized in certain tissues and organs of the body, their particular functions and expression patterns in CNV actually have not been well established. Using the rat CNV model, this study evaluated temporal changes in messenger RNA (mRNA) and protein expression of these three growth factors in both retinal pigment epithelial (RPE)/choroidal and retinal tissues. These temporal expression patterns were compared histologically to areas of immunofluorescence, the proliferation of endothelial cells, neovascular development, and changes in vascular permeability in developing CNV sites.

2. Materials and methods

2.1. Animals

Eighty-four male adult (~250 g) Brown-Norway rats (Charles River Laboratories, Wilmington, MA) were used in this study. All procedures were performed with strict adherence to guidelines for animal care and experimentation prepared by the Association for Research in Vision and Ophthalmology and by the Indiana University Institutional Animal Care and Use Committee. For all procedures, animals received intramuscular (IM) ketamine at 50 mg/kg, xylazine at 5 mg/kg and acepromazine at 1 mg/kg. Topical 1% tropicamide and 2.5% phenylephrine were administered for pupillary dilation and accommodative arrest.

2.2. Laser-induction of CNV

Animals received focal laser photocoagulation to induce CNV formation as described previously (Hu et al., 2005). Briefly, a series of 8 photocoagulation sites were concentrically placed around the optic disk using a diode laser (OcuLight GL, Iris Medical Instrument, Mountain View, CA) of 532 nm wavelength, 0.05 s duration, 75 μ m spot size, and 120 mW power. Although not identical, this well-documented and reliable laser trauma CNV model exhibits many salient pathologic and molecular features of neovascularization clinically found in AMD.

2.3. Tissue processing for traditional mRNA and protein assessments

At designated times after the induction of laser photocoagulation sites (30 and 90 min, 6, 24 and 72 h, 1 and 4 weeks for protein and traditional mRNA analyses plus 60 min, 12 h and 2 weeks for protein analyses), eyes were enucleated from euthanized animals. Nonlasered eyes also were harvested as normal controls for both procedures. Retinal and RPE/choroidal tissues were harvested separately under dissection microscopy. Briefly, the anterior segment was removed surgically, along with as much vitreous as possible. The retina was gently detached from the choroid. The RPE/choroid complex then was peeled away using surgical blades. The tissues from 16 rats were placed immediately in RNAlater solution (Qiagen; Valencia, CA) for RNA isolation. Tissues from another 22 rats were frozen immediately at -80°C for further protein extraction. Samples from both eyes of each animal were combined to obtain the necessary RNA and protein material for analysis at each time point.

2.4. Reverse transcription polymerase chain reaction (RT-PCR) measurements

For traditional RT-PCR measurements, total RNA was isolated from retinal and RPE/choroidal tissues using the RNeasy Mini Kit with DNAase I on-column digestion (Qiagen, Valencia, CA) and following the manufacturer's protocol. Each sample of 2 μ g total RNA was reverse transcribed into 20 μ l cDNA using the Superscript II cDNA synthesis Kit (Invitrogen, Carlsbad, California) and oligo (dT)₁₈ primers (Ambion Inc., Austin, Texas). PCR was performed with 2 μ l cDNA using Platinum Taq DNA polymerase (Invitrogen) in the following conditions: starting with one time of 3 min at 94°C , then denaturing at 94°C for 45 s, annealing at 55°C for 45 s, and extending at 72°C for 60 s, total 32 cycles. The primers were: 5'-CCA TGA ATT TGA CCT CTA TG-3' (sense) and 5'-CTG TAA CCT TCT CCT TGG CC-3' (anti-sense) for HGF; 5'-AGG CTG CAC CCA CGA CAG AA-3' (sense) and 5'-CTT TGG TCT GCA TTC ACA TC-3' (anti-sense) for VEGF; 5'-GGC TTC TTC CTG CGC ATC CA-3' (sense) and 5'-GCT CTT AGC AGA CAT TGG AAG A-3' (anti-sense) for bFGF. For each experiment, β -actin was used as a control gene. All PCR products were electrophoresed on a 1.5% agarose gel. The appropriate product size was determined by comparison with a DNA ladder. The image was captured by the ChemiDoc XRS system (Bio-RAD Laboratories, Hercules, California) and processed with Quantity One analysis software. The intensity of bands obtained by this semi-quantitative method were then exported to an excel spreadsheet where values were expressed relative to the internal β -actin control. Two independently obtained tissue samples were analyzed 3 times for each time point to ensure reproducibility and reliability of the results.

For quantitative real-time qRT-PCR measurements of mRNA expression (two-step method: denature, annealing/amplication), total RNA was isolated from retinal and RPE/choroidal tissues from lasered eyes of 3 rats at designated time points (30 and 60 min, 6,

24, and 72 h and 1 week) and from nonlasered eyes of 3 controls (21 animals total) using the RNeasy Mini Kit with DNase I on-column digestion (Qiagen, Valencia, California) following the manufacturer's protocol. Each RNA sample was analyzed on the Agilent Bio-Analyzer 2100 using an RNA 6000 Nano LabChip and verified that there were sharp bands and peaks for the 28S and 18S ribosomal RNA. RNA samples also were verified so that the ratio of A_{260}/A_{280} was closely around 2.0 and the ratio of A_{260}/A_{230} was greater than 1.7. RNA samples were reverse transcribed into cDNA using the Superscript II cDNA synthesis Kit (Invitrogen, Carlsbad, California) and oligo(dT)18 primers (Ambion Inc., Austin, Texas). Real-time qPCR was performed in triplicate using 50 μ l of reaction mixture containing primer, cDNA (equivalent to 20 ng of total RNA), and SYBR Green Supermix (Bio-Rad, Hercules, California) on a single-color real-time PCR detection system (MyiQ; Bio-Rad). Reactions were started with denaturing at 94 °C for 30 s, annealing and extending at 60 °C for 45 s. The resulting threshold cycle values for all genes were exported to Excel spreadsheet for analysis. Both threshold cycles of the No Template Control and No Reverse Transcription Control were verified to be greater than 35, indicating no DNA contamination in the system. Glyceraldehyde-3-phosphate dehydrogenase (GAPDH) was used as an internal control, and relative levels of HGF, VEGF and bFGF compared with that of GAPDH were calculated. The primers for all real-time qRT-PCR analyses were: CCC AAA TGT GAC GTG TCA AG (forward primer) and ATC CCA AGG AAC GAG AGG AT (reverse primer) for HGF, GCC CAT GAA GTG GTG AAG TT (forward primer) and ACT CCA GGG CTT CAT CAT TG (reverse primer) for VEGF, CCG TAC CTG GCT ATG AAG GA (forward primer) and CCG TTT TGG ATC CGA GTT TA (reverse primer) for bFGF, and GGC ATT GCT CTC AAT GAC AA (forward primer) and TGT GAG GGA GAT GCT CAG TG (reverse primer) for GAPDH. These samples were analyzed 2 times for each time point and these results were verified by an independent laboratory to ensure reproducibility and reliability of the results.

To further clarify the reliability and reproducibility of the previously described two-step qRT-PCR analysis, a second laboratory independently verified the data (not shown) by evaluating the RNA samples from the same eyes using a different qRT-PCR method (iScript One-Step RT-PCR Kit with SYBR Green, Bio-Rad). For additional details about this analysis method, consult [Rajashankar et al. \(2008\)](#).

2.5. Western blot protein analysis

Samples were homogenized in ice-cold lysis buffer containing 1% Nonidet P-40, 0.1% sodium dodecyl sulfate (SDS), 1 mM PMSF, 1 mM sodium orthovanadate (Na_3VO_4), 1 mM NaF, 1 μ g/ml aprotinin, 1 μ g/ml leupeptin, 1 μ g/ml pepstatin, and 50 mM Tris-HCl at pH 7.4. The protein concentration of the resultant supernatants was measured by Bio-Rad protein assay.

The supernatants containing 50 μ g of proteins were resolved on 10% SDS-PAGE polyacrylamide gel under reducing condition with diethiothreitol (DTT) and electroblotted to PVDF membrane. After blocked for 1 h at room temperature in 5% nonfat dry milk in Tris-buffered saline (TBS), the membranes were incubated with goat anti-HGF antibody (R&D Systems, Minneapolis, MN) at a dilution of 1:1000 with 1% nonfat dry milk in TBS for overnight at 4 °C. Horseradish peroxidase (HRP) conjugated anti-goat IgG (R&D Systems) was used as the secondary antibody at a dilution of 1:10,000 for 1 h at room temperature.

For Western blot analysis of VEGF and bFGF, 12% SDS-PAGE polyacrylamide gels were used. Rat VEGF₁₆₄-specific goat IgG (R&D Systems) and rabbit anti-bFGF polyclonal antibody (Advanced Targeting Systems, San Diego, CA) were applied as the primary antibodies at a dilution of 1:1000. HRP-conjugated anti-goat IgG

(R&D Systems) and HRP-conjugated anti-rabbit IgG (Santa Cruz Biotechnology, Santa Cruz, CA) were used correspondingly as the secondary antibodies at a dilution of 1:10,000. These antibody concentration ratios were determined to provide the best signal detection of growth-factor protein isoforms versus background labeling of nonspecific bands. Two independent sample analyses were conducted at each time point to verify the reproducibility of the results.

For each analysis, anti-actin antibody (Sigma-Aldrich, Saint Louis, MI) was used at a dilution of 1:2000 as the control protein. All membranes were incubated with ECL Plus detection reagent (Amersham Biosciences, Piscataway, NJ). The images were captured by the ChemiDoc XRS system, and the intensity of bands was analyzed with Quantity One software. Similar to mRNA analyses, the semi-quantitative data obtained by this method were then exported to an Excel spreadsheet where values were expressed relative to the internal β -actin control. Two independently obtained tissue samples were analyzed 3 times for each time point to ensure reproducibility and reliability of the results.

2.6. Immunofluorescence microscopy of tissue cytokine expression

To remove blood cells/components as potential targets for immunolabeling of cytokines, 7 deeply anesthetized rats were transcardially perfused with 50 ml of phosphate-buffered saline. The eyes were enucleated and fixed in 4% paraformaldehyde at 4 °C overnight, and processed for routine paraffin-embedded sectioning. Serial retinal/choroidal tissue sections (5 μ m thickness) containing laser sites were mounted on Superfrost/Plus slides (Fisher Scientific) and incubated at 58 °C for 2 h. After deparaffinization and rehydration, the sections were boiled in Tris-EDTA buffer (10 mM Tris base, 1 mM EDTA, 0.05% Tween-20, pH 9.0) using a pressure cooker for 2 min, incubated in 0.1% sodium borohydride for 30 min, blocked with 2% bovine serum albumin, 2% normal donkey or goat serum, and 0.5% Triton X-100 in PBS for 30 min, incubated in the primary antibodies (goat anti-HGF, 1:50, and goat anti-rat VEGF, 1:200, R&D Systems, Minneapolis, Minnesota; rabbit anti-bFGF, 1:200, Advanced Target Systems, San Diego, California) at 4 °C for overnight and in the secondary antibodies (Fluorescein [FITC]-conjugated donkey anti-goat IgG or Rhodamine-conjugated goat anti-rabbit IgG, 1:200, Jackson ImmunoResearch, West Grove, Pennsylvania) at room temperature for 45 min. Mounted with a ProLong Gold antifade DAPI reagent (Invitrogen, Carlsbad, California), immunolabeled tissue sections were visualized under an inverted fluorescence microscope (Leica DM IRB, Leica Microsystems Inc., Bannockburn, Illinois). Negative controls were included by omitting the primary antibody to confirm the specificity of the antibodies.

2.7. Histologic tissue preparation

Intravenous (I.V.) administration of a fluorescent albumin dye allowed visualization of general neovascular development and also permitted a general evaluation of interstitial vascular leakage from neovessels at CNV sites. Administration of a fluorescent cationic liposome dye that expresses high affinity binding for negatively-charged new endothelial cells made it possible to observe and evaluate dynamic changes in neovascularization over time ([Krasnici et al., 2003](#)). For *in vivo* colocalization of FITC-albumin (Alexa 488) and rhodamine-cationic liposomes (LipoRed, Munich Biotech AG), 2 rats at times of 3, 6, 9, 12 and 15 days after induction of laser trauma plus 2 nonlasered controls received a slow I.V. injection of 400 μ l total volume, consisting of 5 mg FITC-albumin in 50 μ l rhodamine-cationic liposome stock (9.5 mM lipid/0.5 mM rhodamine) plus 350 μ l of sterile saline. After 15 min of dye circulation, eyes were enucleated.

Eyes were fixed in 4% phosphate-buffered paraformaldehyde solution (2 h at room temperature). For each eye, a single square-shaped tissue block (approximately 8–10 mm/side), of the posterior segment (retina, choroid, sclera), containing the photocoagulation sites and optic disk, were hand-sectioned from the eyecup. The resultant tissue sections for flat-mount confocal microscopic and radial light microscopic analyses were transferred to PBS for direct examination or further immunohistochemical processing.

Tissues from 3 animals at 2 and 7 days after lasering were processed for light microscopic examination. Posterior segments were dehydrated, embedded in paraffin, and serially sectioned (6 μ m thickness). The resultant radial tissue sections were processed with CD31 antibodies for immunolabeling of endothelial cells, with CD68 antibodies for immunolabeling of monocytes and macrophages (DakoCytomation Inc.), or with hematoxylin and eosin for histochemical staining.

2.8. Confocal microscopy

Confocal microscopy was performed using a Zeiss LSM. The scope's krypton/argon laser was set to 30% intensity; the gains and offsets were kept the same for all sample groups. Using a focus motor, 50–75 optical sections were made through whole tissue samples that ranged from 100 to 150 μ m in thickness. As a note, the thickness of tissues increased with post-trauma CNV membrane development. Confocal images were collected such that they transversed the entire thickness of the particular sample though the retina and into the choroid. Images were taken using a 10 \times objective in four quadrants for an entire overview and were taken

with a 20 \times water immersion objective for detailed analyses of individual CNV membrane sites. Images were obtained using Zeiss LSM Browser digital camera software. Subsequently, the four quadrants around the optic disk were brought together in a 3-dimensional montage format using Amira software. Images of individual CNV sites were analyzed for background fluorescence (due to capillary perfusion) and changes in labeled areas of neo-vascularization were evaluated using Metamorph software (Universal Imaging). Detailed 3-dimensional analyses of stacked images were carried out using Voxx software.

2.9. Statistical analysis

Results were expressed as the mean \pm SD. Differences were evaluated by one-way ANOVA using SPSS software (SPSS Inc., Chicago, IL). $P < 0.05$ was defined as statistically significant.

3. Results

3.1. Differential expression of HGF, VEGF and bFGF mRNA in laser-induced CNV

To determine potential changes in the expression of HGF, bFGF and VEGF in laser-induced CNV, mean mRNA expression levels for these 3 growth factors in RPE/choroidal and in retinal tissues were first evaluated and compared at different times after lasering by a traditional reverse transcriptase RT-PCR method and by real-time qRT-PCR. Results from the traditional RT-PCR are shown in Fig. 1. In the RPE/choroidal tissues (Fig. 1A, C), mRNA expression for HGF was

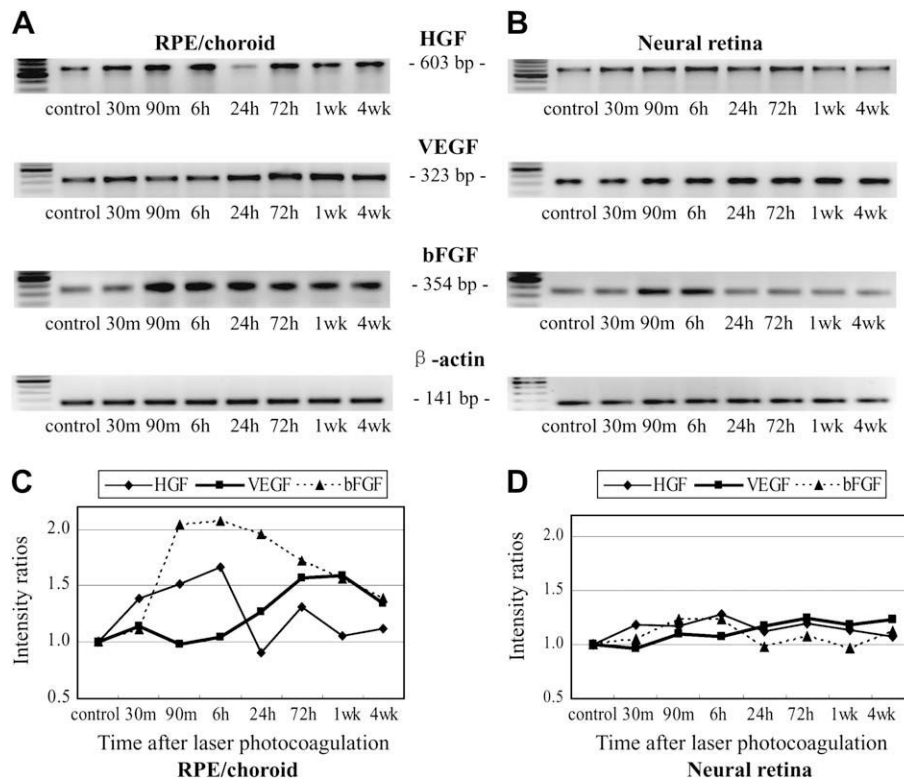


Fig. 1. Differences in messenger RNA expression for HGF, VEGF, and bFGF cytokines were determined by traditional reverse transcriptase RT-PCR at different time points after laser-induction of CNV. In the RPE/choroidal tissues (A, C), HGF mRNA was significantly upregulated after laser photocoagulation, starting from 30 min, peaking around 6 h, decreasing around 24 h, and then elevating again from 72 h to 4 weeks. No significant increase in VEGF mRNA was observed before 24 h. VEGF mRNA peaked around 72 h to 1 week after laser photocoagulation. A significant upregulation of bFGF mRNA was noticed from 90 min, and the level was decreased but still higher than the control level after 24 h through 4 weeks. In the retinal tissues (B, D), the mRNA levels for HGF, VEGF and bFGF were not significantly changed after laser photocoagulation. HGF mRNA was slightly elevated, and was roughly the same at all time points. The mRNA level for VEGF was slightly increased after 24 h through 4 weeks. A small upregulation of bFGF mRNA was also noticed from 90 min to 6 h (C, D). Intensity ratios of HGF, VEGF and bFGF bands were compared to the internal control, β -actin. Two independently obtained tissue samples were analyzed 3 times for each time point to ensure reproducibility and reliability of the results.

substantially upregulated by 30 min (as denoted by a 39% increase in the relative intensity, $P < 0.05$), peaked at around 6 h (67% intensity increase relative to that of the control baseline, $P < 0.05$), decreased slightly below the baseline level at 24 h, increased again to a secondary peak (31% relative increase, $P < 0.05$) at around 72 h, and then returned to around baseline for the remainder of the 4-week period. Similarly, a rapid upregulation of bFGF mRNA occurred after lasering, which doubled in expression (104–107% relative increase, $P < 0.05$) compared to baseline at its peak around 90 min to 6 h; subsequently, values slowly decreased but remained above baseline during the period from 1 week to 4 weeks ($P < 0.05$). After laser photocoagulation, VEGF mRNA expression generally remained unchanged through 6 h, then gradually increased to peak (57–59% relative increase, $P < 0.05$) during the period between 72 h and 1 week and, similar to bFGF, was still elevated at 4 weeks.

In retinal tissues (Fig. 1B, D), increases in mRNA expression for these three growth factors remained small in comparison to changes measured in the RPE/choroidal tissues; maximum expression for each growth factor (23–28% relative increase) was comparable to the other two. Nevertheless, small temporal differences in expression were discernable. HGF mRNA levels increased somewhat after lasering (achieving a 28% relative increase at 6 h) and then remained partially elevated for all subsequent time points. A small transient elevation (23% relative increase) of bFGF mRNA expression occurred from 90 min to 6 h after lasering and then returned to baseline. Expression of VEGF mRNA increased to a maximum at 72 h (25% relative increase) and continued along a low-level plateau for the remainder of the 4-week period.

Results from real-time qRT-PCR to evaluate mean mRNA expression differences are shown in Fig. 2. Subtle increases in RPE/choroidal expression of HGF mRNA within the first 6 h after

lasering, and subsequently a larger increase was measured at 2 weeks post-laser. Unfortunately, no statistically significant findings were found. In the neural retina, expression at all time points approximated the control values.

For VEGF expression of mRNA, qRT-PCR indicated a significant increase (>2 fold difference) at 1 week post-laser in the RPE/choroidal tissue samples (Fig. 2). In the neural tissue samples, this method demonstrated a small but significant increase at 30 min, while at 6 h a much larger increase (>16 fold difference compared to control) was measured.

Large statistically significant increases (>6 fold difference) in bFGF mRNA expression were demonstrated at 6 h in both the RPE/choroidal and neural retinal samples (Fig. 2). Significant, but reduced expression continued to be measured at 24 h in the neural retinal samples. In addition, a secondary increase (>2 fold difference) in bFGF mRNA expression was detected at 1 week in the RPE/choroid (Fig. 2).

3.2. Western blot analysis for HGF, bFGF and VEGF

To confirm the mRNA data and to directly compare the protein expression of HGF, VEGF, and bFGF, Western blot analysis was performed. HGF and bFGF upregulated quickly and reached their peak expression levels within hours, as compared to days for maximum VEGF expression. Increases in precursor and activated HGF isoforms and a low-molecular weight bFGF isoform were measured, but VEGF isoforms within RPE/choroid initially were not detected.

HGF is secreted as an inactive precursor form, and becomes two active subunits after cleavage by serine protease. In RPE/choroidal tissues (Fig. 3A, C), maximum levels of HGF protein were expressed

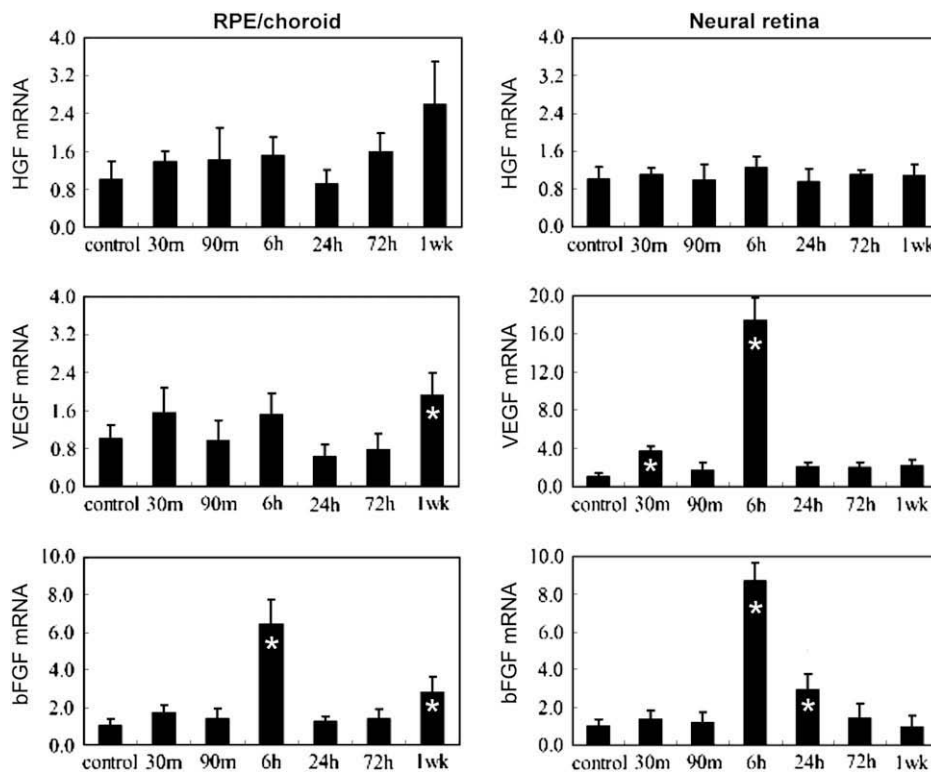


Fig. 2. Differences in messenger RNA expression (fold differences) of HGF, VEGF, and bFGF cytokines were determined by quantitative real-time qRT-PCR at different time points subsequent to laser-induced CNV. Statistically significant ($P < 0.05$) increases in mRNA expression are designated by asterisks. Samples from 3 animals were analyzed 2 times for each time point. No increase in expression was found for HGF. VEGF demonstrated a significant increase in the retinal samples at 30 min and 6 h, while in the RPE/choroid a significant increase occurred at 1 week. Significant increases in bFGF expression occurred in the RPE/choroid at 6 h and again at 1 week, while in retinal tissues increased expression was found at 6 h and 1 week. Further verification of these data was provided by an independent laboratory, using the same sample sources, but a slightly different qRT-PCR method of analysis.

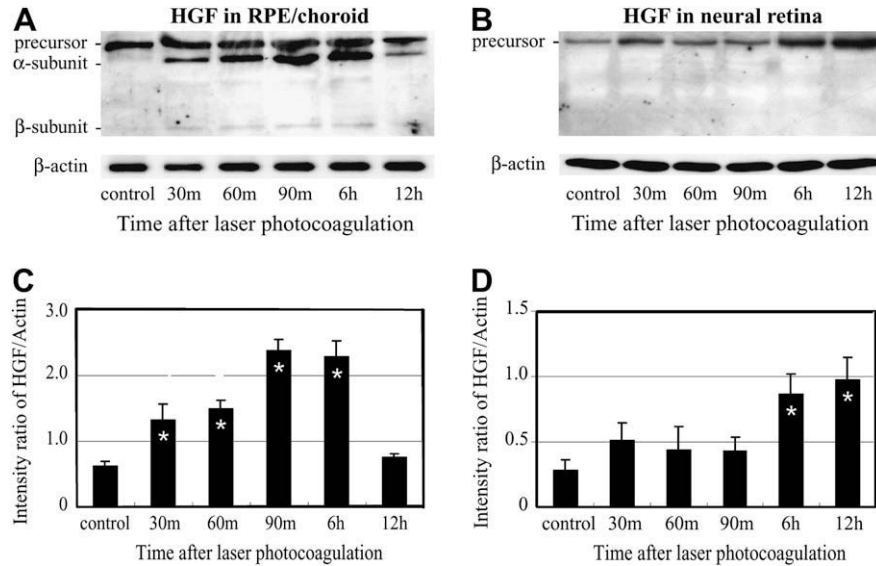


Fig. 3. Western blot analysis of HGF in laser-induced CNV. In RPE/choroidal tissues (A), maximum levels of HGF protein occurred between 90 min and 6 h after laser photocoagulation, and three distinct bands of approximately 69, 54 and 30 kDa were present, corresponding to the precursor, α - and β - subunits of HGF respectively. The α - and β - subunits of the activated form of HGF were apparent from 30 min, peaked between 90 min and 6 h, and stayed noticeable through 72 h (images after 12 h not shown). The graph (C) illustrates the ratio of relative HGF intensities, as the sum of all of three bands for the nonlasered control and at each time point, as compared to β -actin. In retinal tissues (B, D), HGF protein levels increased at 30 min after laser treatment, peaked between 6 and 12 h, and then stabilized at a slightly lower level through 72 h (images after 12 h not shown). Only the precursor form of HGF was observed in retinal tissues. Differences between each time point compared to the nonlasered control were evaluated statistically by one-way ANOVA testing, asterisk indicating $P < 0.05$.

at 90 min and 6 h after lasering, and three distinct bands at apparent molecular weights (MW) of 69, 54 and 30 kDa were present. The 54 and 30 kDa bands, that correspond to the α - and β -subunits of activated HGF, were upregulated by 30 min (constituting a 111% mean increase in expression compared to the control HGF protein level, $P < 0.05$), achieved peak expression between 90 min and 6 h (262–278% mean increase, $P < 0.05$). After 12 h, HGF α - and β - subunits were no longer detectable, although elevated levels of the precursor protein slowly regressed to approximately 20% above baseline during the period from 12 to 72 h.

Meanwhile in retinal tissues (Fig. 3B, D), only one major HGF isoform of 69 kDa MW was expressed, which corresponded to its precursor form. HGF protein levels had increased by 82% over

baseline at 30 min after lasering, peaked between 6 and 12 h (207–246% increase, $P < 0.05$), and then stabilized at a slightly lower level (103% above baseline) through 72 h before returning to baseline at 1 week.

In RPE/choroidal tissues (Fig. 4A, C), only the 14 kDa low-molecular weight (LMW) isoform of bFGF was expressed during blot analyses. Upregulation was apparent by 30 min (231% increase compared to baseline expression, $P < 0.05$). Protein expression maximized (an increase of 472% over baseline, $P < 0.05$) during the period from 90 min to 12 h and then slowly decreased, but remained at elevated levels through 1 week.

Unlike the RPE/choroidal tissues, in retinal tissues (Fig. 4B, D) bFGF proteins were expressed as multiple bands of 14, 18, 21, and

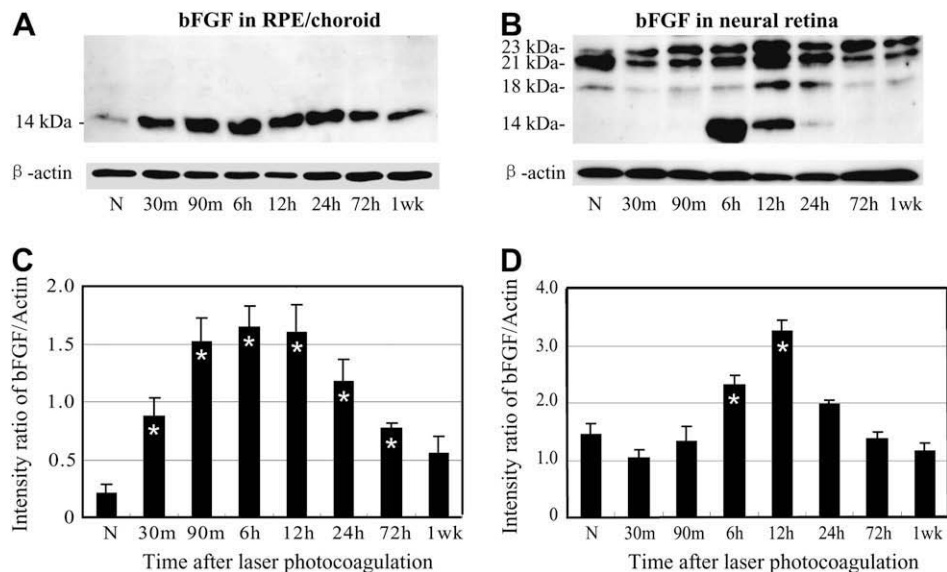


Fig. 4. Western blot analysis of bFGF in laser-induced CNV. In RPE/choroidal tissues (A, C), only a 14 kDa band was observed. Basic FGF expression increased from 30 min, maximized around 6 h and maintained a higher level through 1 week. Basic FGF protein was expressed as multiple bands of 14, 18, 21 and 23 kDa in retinal tissues (B, D). The total protein of bFGF peaked around 12 h. A low-molecular weight band of approximately 14 kDa was observed only from 6 to 24 h. Asterisk indicated $P < 0.05$.

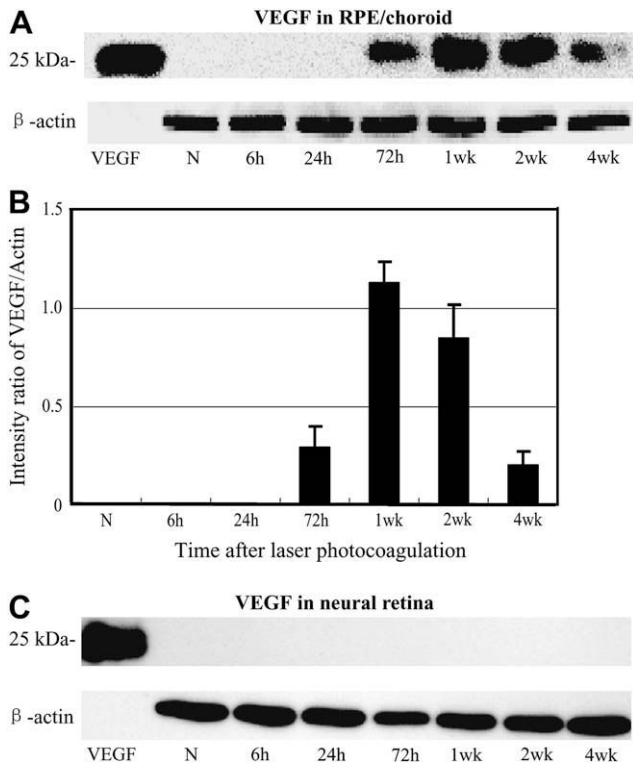


Fig. 5. Western blot analysis of VEGF in laser-induced CNV. In RPE/choroidal tissues (A, B), VEGF occurred as a single band of 25 kDa at 72 h after laser photocoagulation, peaked around 1 week, and then was expressed at lower levels through 4 weeks. VEGF protein was not detectable by this antibody in retinal tissues (C).

23 kDa. The composite mean expression of all bFGF proteins peaked around 12 h (126% increase compared to baseline, $P < 0.05$) and returned to slightly above baseline by 24 h. However, peak expression of the 14 kDa LMW isoform of bFGF in the retina selectively occurred at 6 h, instead of at 12 h. Peak expression of the 14 kDa isoform at 6 h corresponded to a point midway through the broader time period when this particular isoform was maximally expressed in the RPE/choroid. Within the retina, however, expression of the 14 kDa isoform had decreased by 12 h and was measurable only through 24 h, as compared to the continued protein expression for this particular isoform at 1 week in RPE/choroidal samples.

VEGF protein levels in RPE/choroidal tissues (Fig. 5A, B) were below detectable limits in nonlasered control samples, as well as in eyes at 6 and 24 h after induction of laser photocoagulation sites. VEGF protein expression, as a single band of 25 kDa, was first measured at 72 h after lasering, peak expression occurred around 1 week, continued to be well-expressed at 2 weeks, and then decreased to a much lower level at 4 weeks. In retinal tissues (Fig. 5C), VEGF protein levels remained below the detectability of this antibody method at all of the sampled time points.

3.3. Immunofluorescence studies of HGF, VEGF, and bFGF

Immunolabeling of radial tissue sections for HGF with green fluorescein isothiocyanate (FITC) fluorescence exhibited intense labeling shortly after the induction of laser lesions. At 6 h post-laser (Fig. 6A, arrow), intense and focal HGF labeling was localized within the choriocapillaris of lesion sites. By 72 h, and again at 1 week (Fig. 6B, C), this labeling had almost disappeared, with only intermittent staining around the developing CNVM. A somewhat similar

result was observed for bFGF immunolabeling with red rhodamine fluorescence. Intense, localized immunolabeling (Fig. 6G, arrow) of the choroid and particularly the choriocapillaris occurred within the region of the lesion site at 6 h. At 72 h and 1 week (Fig. 6H, I), labeling had diminished and was more diffuse within the developing and expanding CNVM.

Immunolabeling (with FITC fluorescence) for VEGF was interesting because at 6 h very little labeling was present within the central lesion site as noted with HGF and bFGF. Instead, intense VEGF staining was localized to the region immediately adjacent to the lesion site (Fig. 6D, arrows) and could be attributed to distal Müller cell processes. At 72 h, Müller cells continued to be labeled, but not as intensely (Fig. 6E, arrows) as at 6 h. In addition, sub-retinal labeling now had become evident within the developing CNVM. At one week, VEGF labeling in and around the CNVM had diminished (Fig. 6F).

3.4. Histologic time course of CNV development and vascular perfusion

To better understand the potential relationships between expression patterns and functions, the differential expression of these three growth factors were compared to the histologic proliferation of endothelial cells, neovascular development, and temporal changes in vascular permeability at laser-induced CNV sites.

Neovascular formation and increased endothelial cell labeling already could be identified at developing CNV sites with light and confocal microscopy by 2–3 days after induction of laser trauma (Figs. 7 and 8). The presence of new endothelial cells was evident by fluorescent labeling with cationic liposomes at 3 days within the central trauma site as well as in neovessels that were expanding tangentially beyond the newly-formed CNV membranes (Fig. 8). Neovascular activity was most prominent within the central (lasered) portion of the CNV site at 3 days (Fig. 8A).

At 6 days, angiogenic endothelial cell labeling had continued within the central site and along newly-formed vessels (Fig. 8B), but in addition, a ring of labeled cells was obvious around the expanding circumference of the CNV membrane. By day 12, maturing vessels had established a network lattice appearance and some had further expanded asymmetrically to establish vascular connections with neovessels in neighboring CNV sites (Fig. 8C). As summarized in Fig. 9A, liposomal labeling intensified at 3 days, peaked dramatically around 6 days, and then fell off slightly to a plateau level that continued until at least day 15. Measurements of interstitial albumin, denoting vascular filling and leakage (Fig. 9B), initially peaked at 3 days, decreased at 6 days, reintensified to a secondary peak at 12 days, and then decreased to near baseline levels at 15 days.

In mature CNV sites, ~4 weeks after lasering, the presence of 1–3 chorioretinal anastomoses typically can be identified and traced within consecutive serial radial-tissue sections. In this temporal study, developing anastomotic vessels were observed in radial tissue sections at 2–3 days after lasering, a much earlier time than anticipated (Fig. 7B, D). Surprisingly, 3-dimensional reconstructions of several CNV sites, with confocal microscopy, revealed that numerous anastomoses (varying from 10 to 20 per site) had formed both at and adjacent to the CNV membranes (Fig. 10).

4. Discussion

This investigation produced unexpected findings and demonstrated the complexity of the angiogenic process in this choroidal neovascular model. Table 1 summarizes the comparative similarities and differences noted in this current study by the different qualitative and semi-quantitative methods for cytokine

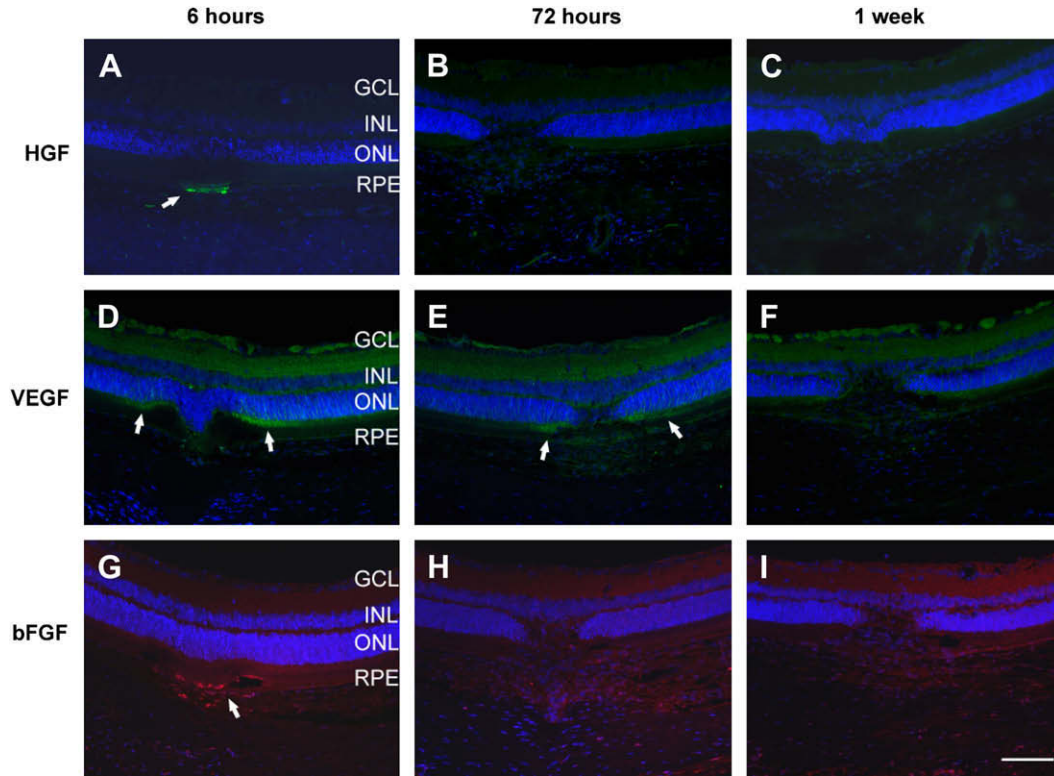


Fig. 6. Immunofluorescent labeling of HGF, VEGF and bFGF expression at 6 h, 72 h and 1 week after laser trauma. Note the localized labeling within the choroid of lesion sites for HGF (A, arrow) and bFGF (C, arrow) at 6 h. Alternately, VEGF immunolabeling was present at 6 h in Müller cells located adjacent to the lesion site (D and E, arrows). VEGF labeling first becomes noticeable within the developing CNVM at approximately 72 h (E). Bar = 75 μ m.

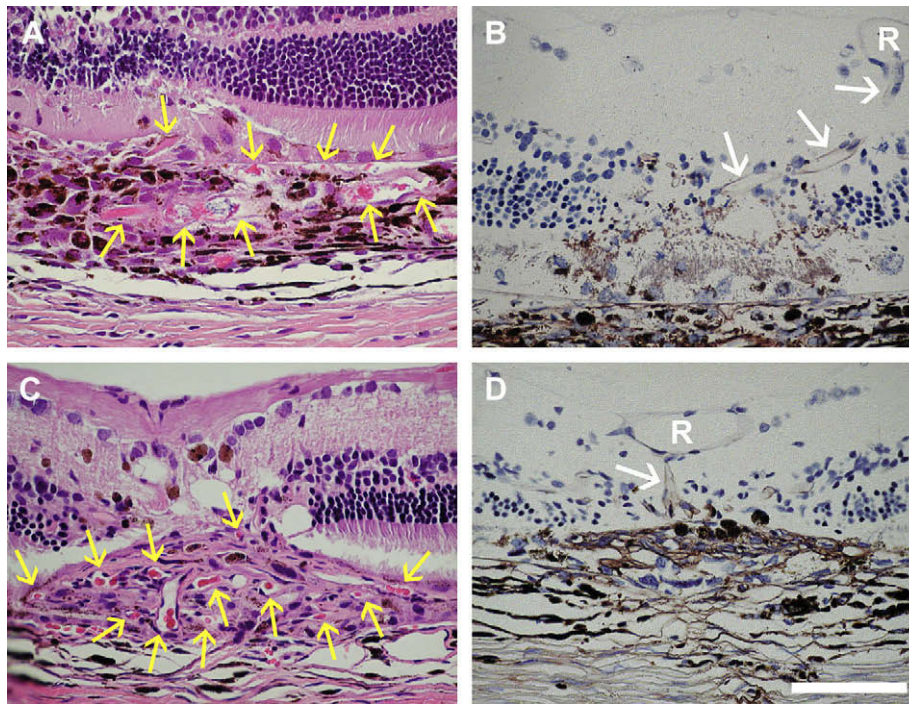


Fig. 7. Comparison of developing CNV sites in radial tissue sections. Early vascular development (yellow arrows) within the newly forming CNV membrane already is observed at two days (A) after lasering in hematoxylin and eosin stained tissues and increased vascular maturation is evident by 7 days (C). CD-31 immunolabeled endothelial cells (brown) are diffusely labeled within the initial CNV membrane against a methylene-blue stained background at 2 days post-laser (B), while more sophisticated lattice-like structuring of labeled vessels is apparent at 7 days (D). Note also the early presence of anastomotic vessels (white arrows), forming between the CNV membrane and retinal blood vessels (R), discernable at both 2 days (B) and 7 days (D) in tissue sections located just peripheral to the central laser trauma site. Infiltrating monocytes/macrophages also are evident in and around CNV sites at both time points (A–D) and have been identified by CD-68 immunolabeling (not shown). Bar = 75 μ m.

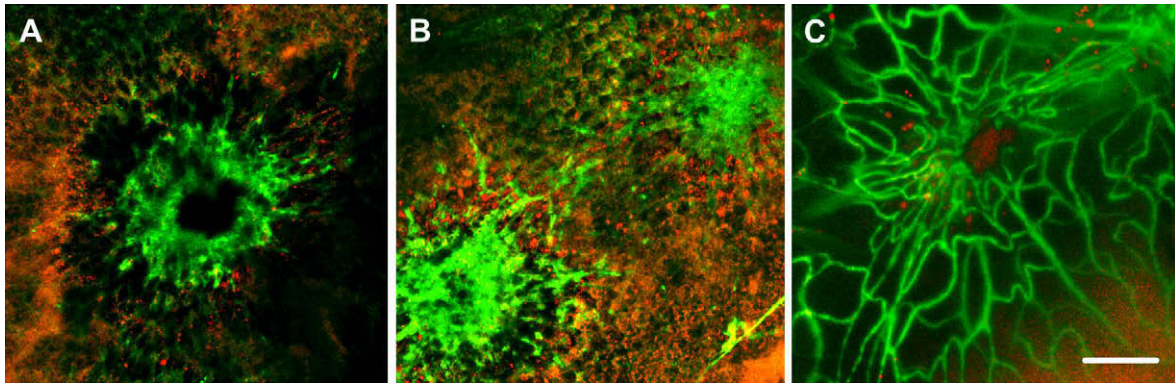


Fig. 8. Fluorescence confocal microscopy of CNV sites (flat-mount views) at (A) 3 days (B), 6 days, and (C) 12 days after lasering with rhodamine-cationic liposome (red) labeling to indicate new endothelial cells/angiogenic activity and with FITC-albumin (green) labeling of vessels and leakage. (A, B) Images were obtained at the depth of the junction between the photoreceptors (honeycombed in appearance; at upper left of figs.) and the retinal pigment epithelium cells (mossy in appearance and orange-brown in color; at lower right in figs). (C) Image is at the level of the choriocapillaris. At 3 days (A) note the neovascular development and leakage around the central trauma site with some early collateral vessels (green labeled for albumin) and circumference around the central site (punctuated, bright red liposomal labeling) indicative of expanding neovascularization. At 6 days (B) continued lateral expansion of the neovascular membrane (red liposomes), vascular maturation, and the formation of collateral processes (green) were evident between adjacent CNV sites. By 12 days (C) neovascular development still continued within the central membrane (red) and further differentiation of maturing peripheral vessels (green) was apparent peripherally. Bar = 75 μ m.

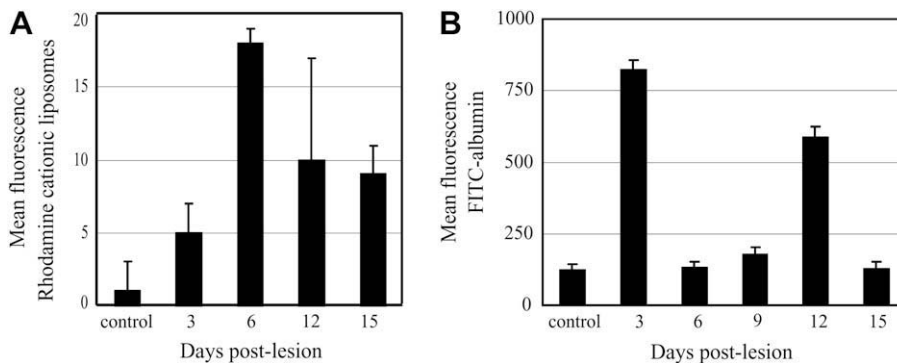


Fig. 9. Graphical expression (A) of changes in new endothelial cells in control (nonlasered) and at successive post-induction time points in lasered eyes. Angiogenic endothelial cells (negatively-charged) were labeled with rhodamine-cationic liposomes (red). Note that peak labeling occurred at 3 days after laser-induction of CNV sites (see also Fig. 7B). Semi-quantitative analyses of changes in rhodamine mean total fluorescence (i.e., pixel intensity; $n = 4$ samples per each control/time point) in confocal fluorescence images were performed using Vioxx and Metamorph software. Graphical expression (B) of changes in FITC mean thresholded fluorescence (i.e., pixel intensity; $n = 4$ samples per each control/time point) denoting vascular filling and leakage in control (nonlasered) and at successive post-induction time points in lasered eyes with FITC-albumin labeling. The initial increase at 3 days may depict a combination of edema from the laser trauma site and leakage from early neovascularization; whereas the secondary spike at 12 days may represent possible vascular hyperperfusion by maturing blood vessels.

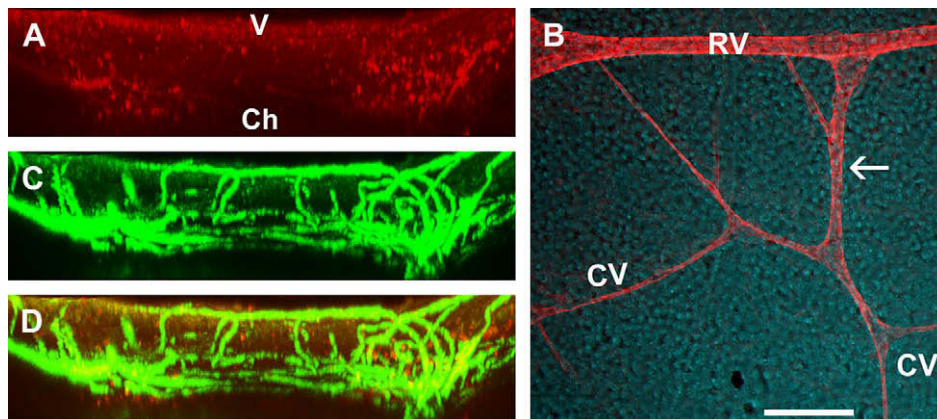


Fig. 10. Confocal microscopy illustrating radial views (A, C, D) of multiple anastomotic vessels that formed by 12 days after lasering at and near two adjacent CNV membrane sites and a flat-mount, composite 3D view (B) of a single anastomosis at 12 days post-laser that was located adjacent to a CNV membrane. Fluorescence demonstrates: (A) cationic liposomal (red) labeling of angiogenic endothelial cells; (B) anastomotic vessel (arrow) connecting a large-diameter retinal vessel above with choroidal vessels below; (C) FITC-albumin (green) labeling of vessels; and (D) extent of CNV development (yellow fluorescence) by integrating images of both (A, C) fluorescent labels. V: vitreous; Ch: choroid; RV: retinal vessel; CV: choroidal vessel. Bar (A, C, D) = 50 μ m; (B) = 25 μ m.

Table 1
Comparison of cytokine activity in the choroid and retina at different time points after laser-induction of choroidal neovascularization using different qualitative and semi-quantitative methods of evaluation. Values in parentheses represent times and locations of maximum expression or labeling. Values designated with **bold** lettering are statistically significant ($P < 0.05$).

Cytokine	bFGF		HGF		VEGF	
	RPE/Choroid	Retina	RPE/Choroid	Retina	RPE/Choroid	Retina
Traditional RT-PCR	30 min–72 h (6 h)	6 h (12 h)	30 min–6 h (90 min)	6 h (12 h)	(1 week)	
Real-time qRT-PCR	(6 h) 1 week	(6 h) 24 h			(1 week)	30 min (6 h)
Protein (western analysis)	(6 h)		(6 h)		(1 week)	
Immunofluorescence	(6 h Within choriocapillaris lesion site) 72 h & 1 week in CNVM		(6 h Within choriocapillaris lesion site) 72 h & 1 week in CNVM		72 h & 1 Week in CNVM	(6 h in Müller cells)

identification and expression. After trauma to Bruch's membrane, increased growth factor expression in the RPE and choroid were expected; however, individual differences characterized each cytokine. Within 6 h, all three cytokines demonstrated increased mRNA expression, but there were differences as to where upregulation occurred (choroidal samples for HGF and bFGF, retinal samples for VEGF). At 6 h, immunolabeling for HGF and bFGF was localized to the choroidal region within laser lesion sites. During this same time, HGF and bFGF also exhibited early protein upregulation. Meanwhile, at 6 h, VEGF appeared confined to Müller cells located immediately adjacent to the lesion site and was first observed in the developing CNVM at 72 h. In this model, early neovascularization within the developing CNV membrane becomes histologically evident (to us and others) by 2–3 days after trauma (Edelman and Castro, 2000). Expression of VEGF protein was first measurable at 72 h and did not peak until 7 days. Although an increase in VEGF protein was not detectable until 3 days after laser, some level of upregulation probably occurred nevertheless during this time, but detection remained below threshold sensitivity. In addition, the antibody used was selective for the VEGF₁₆₄ isoform. Therefore, how should the results about VEGF from this investigation be interpreted and how might this undetectable increase in VEGF expression be related to the overall initiation and mediation of angiogenic processes during this time period? While this may depend partially upon VEGF potency, a definitive answer simply is not available. These data do not imply that VEGF is uninvolved in early CNV formation, but they do bring into question the relative role of VEGF early in this process. One possibility might be that other more soluble isoforms of rat VEGF (e.g., VEGF₁₂₀) could conceivably be involved in a rapid response by the Müller cells to provide neuroprotection to the photoreceptors following laser injury.

At low concentrations, VEGF has been reported to promote microvascular endothelial cell proliferation by a phosphorylative response via the cellular ERK and MAPK pathways (Cai et al., 2006). At least in this rat model, the early involvement of VEGF would seem to rely principally on pre-expressed levels of soluble VEGF₁₆₄ and, to a lesser extent, possibly VEGF₁₂₀, as well as membrane bound isoforms (i.e., VEGF₁₄₄ and VEGF₁₈₈) that could be cleaved as an activated but less potent VEGF₁₁₀ isoform. During this initial phase of neovascularization exogenous VEGF could participate, as also could HGF and bFGF, as a signaling molecule for vascular CEC recruitment and migration to CNV sites (Asahara et al., 1999; Papetti et al., 2003; Gerritsen, 2005; Wang et al., 2005). In culture, VEGF can increase the number of CECs in a dose-dependent manner (Imanishi et al., 2003); however, soluble VEGF functions as a chemotactic gradient for transmigration of choroidal endothelial cells across the RPE monolayer, which suggests that other growth factors may subsequently be necessary for endothelial cell proliferation (Geisen et al., 2006). Obviously, angiogenesis is not mediated singularly by only one growth factor, but rather from the integrated activities of many regulatory molecules. VEGF, HGF, and/or bFGF can function synergistically to evoke and drive angiogenesis.

HGF demonstrates maximum potency for angiogenesis in the presence of bFGF and VEGF (Schmidt et al., 1999; Gerritsen, 2005). HGF stimulates VEGF expression in many cells and induces VEGF transcription through an increased phosphorylation of transcriptional factor Sp1 (Gille et al., 1998; Wojta et al., 1999; Reisinger et al., 2003). The combination of HGF and VEGF, which results in the cooperative activation of different signaling pathways (Gerritsen et al., 2003) may have an additive or greater effect on endothelial cell proliferation, a synergistic effect on endothelial cell migration *in vitro*, and increased neovascularization in the rat corneal assay (Van Belle et al., 1998; Xin et al., 2001; Gerritsen, 2005).

Current findings, that activated isoforms of HGF were first detected in the RPE/choroid during the first several days after laser, suggest that HGF may play an early regulatory role in CNV development. In various tissues and organs, HGF exhibits pleiotropic angiogenic functions including proliferation, migration, and morphogenesis (Bhargava et al., 1992; Liou et al., 2002; Kuhlmann et al., 2005). Although expressed predominantly by, but not limited to, cells of stromal origin (Birchmeier et al., 1995), sources of ocular HGF include fibroblasts, vascular smooth muscle cells, glial cells, retinal microvascular endothelial cells, ganglion cells, and RPE cells (Koochekpour et al., 1997; He et al., 1998; Lashkari et al., 1999; Cai et al., 2000; Shibuki et al., 2002). HGF is considered more potent in the proliferation of endothelial cells as compared to other factors, including VEGF, bFGF and interleukin-6 (Bussolino et al., 1992; Nakamura et al., 1996). HGF mediates the expression of the cell adhesion molecule, vascular endothelial cadherin, which consequently stimulates endothelial cell motility, migration, and angiogenesis (Martin et al., 2001). HGF stimulates growth and migration of endothelial cells *in vitro* (Rosen et al., 1991; Bussolino et al., 1992; Kuhlmann et al., 2005), and potently induces angiogenesis both *in vitro* and *in vivo* (Grant et al., 1993; Rosen et al., 1993b) HGF-induced endothelial cell growth is augmented by bFGF (Nakamura et al., 1996).

Similarly, the early upregulation and persistence of bFGF expression in this model suggests that it too may be an initial and possibly continuing mediator of CNV development. Basic FGF is produced by a variety of cell types in culture, immunohistochemical, and *in situ* hybridization studies, including vascular endothelial cells of the choriocapillaris, fibroblasts, smooth muscle cells, astrocytes, and RPE cells (Schweigerer et al., 1987; Amin et al., 1994; Matsushima et al., 1996; Ohsato et al., 1997; Martin et al., 2004; Gerritsen, 2005; Rosenthal et al., 2005). Basic FGF is found in extracellular matrix (ECM) from which it can be released by ECM-degrading enzymes such as serine proteases and metalloproteases (Vlodavsky et al., 1987). Basic FGF induces the secretion of VEGF and HGF by Müller glial cells and stimulates cell proliferation (Garcia and Vecino, 2003; Hollborn et al., 2004; Rosenthal et al., 2005). As with VEGF and HGF, neovascularization involves integrated VEGF and bFGF signaling (Tobe et al., 1998; Rosenthal et al., 2005). Maximum co-labeling of VEGF and bFGF in rat RPE and choriocapillaris cells occurs within CNVM sites between 2 and 7 days after laser (Frank, 1997).

Rat bFGF typically occurs in three isoforms, a low-molecular weight (LMW) form of 18 kDa and two high molecular weight

forms (21, 23 kDa), representing alternative translation products from a single mRNA (Müller-Ostermeyer et al., 2001). The 18 kDa isoform occurs mainly in the cytoplasm, whereas the 21/23 kDa bFGF are localized in the nucleus (Claus et al., 2003). In this current study, all three isoforms of bFGF were expressed in the retinal tissues. In addition, a less typical 14 kDa low-molecular weight (LMW) isoform of bFGF was detected in retinal tissue samples between 6 and 24 h after laser photocoagulation, whereas this isoform was the only band detected in RPE/choroidal tissue samples. Others have reported this bFGF LMW isoform in the rat retina after retinal vein occlusion, as well as in the rat brain and in hepatoma cells (Klagsbrun et al., 1987; Powell and Klagsbrun, 1991; Hayashi et al., 1999). The functional significance of this LMW bFGF remains unknown. Because a variety of protease inhibitors were used procedurally to prepare samples for analyses, the 14 kDa LMW isoform of bFGF could have been derived *in vivo* by retinal and choroidal proteases and possibly could represent a proteolytic byproduct of bFGF.

Interestingly, differences in the temporal expression of growth factors are not unprecedented. In a rat ischemic injury model, mRNA expression for VEGF and its receptor decreased immediately and at 6 h after ischemic injury, but returned to control levels by 24 h; whereas immunohistochemistry revealed that VEGF was first evident in endothelial cells after 24 h (Ogata et al., 1998). Meanwhile, RT-PCR analyses revealed that gene expression of bFGF peaked at 6–12 h while FGF receptor expression peaked at 3–12 h (Miyashiro et al., 1998). Likewise, a 3-fold increase in HGF expression was measured at 6 h which remained highly elevated for a period from 48 h (by RT-PCR) to 96 h (by Western blot). Corresponding immunohistochemistry revealed increased HGF labeling of RPE cells at 6 h and in several retinal locations by 24 h (Shibuki et al., 2002).

Previously with a rat laser CNV model, increased expression of bFGF was detected by *in situ* hybridization and immunohistochemical labeling in “RPE-like” and proliferating RPE cells, migrating macrophages, fibroblast-like” cells and choroidal vascular endothelial cells at sampling times from 3 days to 2 weeks after lesion induction (Ogata et al., 1996; Yamamoto et al., 1996a,b). An initial report employing RT-PCR and immunohistochemistry indicated that VEGF expression was comparable to control levels at the “early stage” of laser-induced CNV development; moderate VEGF immunostaining of the choriocapillaris was detected after 1 day, RPE cells and macrophages within the lesion site were labeled at 3 days and 1 week, and RPE cells continued to exhibit staining at 4 weeks (Yi et al., 1997). Recent ELISA and RT-PCR studies with the murine laser CNV model described low VEGF expression at 24 h, which increased on days 3 and 5, and then decreased or returned to baseline values by 7 days (Bora et al., 2005, 2006).

In the current investigation, evaluation of albumin-labeled vasculature and leakage using confocal microscopy indicated that an initial increase in staining was measured at 3 days after laser-induction (Fig. 9B) and this increase may correspond to initial trauma-induced edema as well as leakage from the initially-developing CNV. The substantial increase in albumin staining at approximately 12 days after laser is more intriguing because it may represent a time, just after peak expression of VEGF, when permeability of maturing CNV is increased.

Recent investigations have proposed that two processes, post-natal vasculogenesis and angiogenesis, underlie CNV development (Espinosa-Heidmann et al., 2003, 2005; Sengupta, N., et al., 2003; Csaky et al., 2004; Chan-Ling et al., 2006; Sheridan et al., 2006). During the first three days of neovascular development, the onset of endothelial cell infiltration and proliferation result from CEC and endothelial precursor cell recruitment from the blood stream through a rapid postnatal vasculogenic response. Blood-derived macrophages from circulating monocytes and smooth muscle cells

derived from vascular precursor cells also are important in early neovascularization (Espinosa-Heidmann et al., 2003, 2005; Caicedo et al., 2005). This process then decreases as resident cells continue neovascular development through angiogenesis (Murayama and Asahara, 2002; Sheridan et al., 2006). Angiogenic mediation of resident cells for CNV development begins slowly, but increases over time and sustains neovascularization to completion. The two processes achieve parity at approximately 1 week into neovascular development (Espinosa-Heidmann et al., 2005). While many factors may help regulate both processes, their relative contributions to each process may be different, just as functional differences also may exist during neovascularization in different ocular (choroidal, retinal, corneal) and other bodily tissues (Rousseau et al., 2003; Campochiaro, 2006). The mRNA and protein expressions, in conjunction with immunofluorescence data suggest that bFGF and perhaps HGF may be involved postnatal vasculogenic and possibly extend into angiogenic phases of neovascularization; unfortunately, their regulatory functions and whether these roles might change with time is unknown. Results from this investigation seem to suggest that early maximal expression of bFGF, in conjunction with HGF and soluble VEGF, may serve as initial regulators of neovascularization in this CNV model, whereas the subsequent peak protein expression of VEGF₁₆₄ at 7 days may correspond more appropriately to CNV maturation, stability, and survival, or to regulation of CNV hyperpermeability (Issbrücker et al., 2003).

Meanwhile, in retinal tissues, protein upregulation of cytokines, particularly bFGF, also was an unusual result. Moreover, the retinal expression of precursor HGF and multiple molecular weight isoforms of bFGF, as compared to those isoforms expressed in the RPE/choroid, suggest that retinal vascular homeostasis may be influenced by distal RPE/choroidal changes. Conceivably, the heightened expression of certain growth factors within both the RPE/choroid and their precursors within the retina may contribute to the rapid and proliferative formation of anastomoses between the two vascular networks.

These current findings represent only one step in specifically defining the complex roles of growth factors in the initiation and progression of CNV. Additional studies are needed to fully characterize the diverse and interactive roles of VEGF, HGF and bFGF, as well as the multitude of other growth factors, extracellular matrix proteins, and receptors that participate in CNV development (Eichler et al., 2006). This information is crucial in determining which regulators should be selectively targeted therapeutically, in order to achieve the most beneficial outcome for neovascular AMD patients at different time points in CNV progression (i.e., to inhibit mitogenic initiation of neovascularization, to interrupt and destabilize vascular development, or perhaps to bring vascular permeability under control in already established neovessels).

Acknowledgments

The authors thank Lisa L. Bird-Turner for her technical assistance during this study. The authors thank Dr. Uwe Michaelis, Munich Biotech AG, for generously providing the rhodamine-cationic liposomes. Confocal microscopy and image analyses were performed at The Indiana Center for Biological Microscopy, Indiana University School of Medicine. Voxx software for three dimensional analyses of confocal stack images was developed by Jeff Clendenen and Jason Byars, The Indiana Center for Biological Microscopy.

This study was supported by a grant from the Indiana Center for Vascular Biology and Medicine/Cryptic Masons Medical Research Foundation, by an unrestricted grant from Research to Prevent Blindness, Inc., New York to the Department of Ophthalmology, Indiana University, by the Craig Family Memorial Gifts and by the generosity of Mr. and Mrs. Arthur R. Whale.

Portions of this study were previously presented at the 2003 through 2005 annual meetings of the Association for Research in Vision and Ophthalmology in Ft. Lauderdale, Florida, USA.

References

- Amin, R., Puklin, J.E., Frank, R.N., Kida, I., Moriguchi, A., Matsumoto, A., Matsumoto, K., Nakamura, T., Kaneda, Y., Higaki, J., Ogihara, T., 1994. Growth factor localization in choroidal neovascular membranes of age-related macular degeneration. *Invest. Ophthalmol. Vis. Sci.* 35, 3178–3188.
- Aoki, M., Morishita, R., Taniyama, Y., 2000. Angiogenesis induced by hepatocyte growth factor in non-infarcted myocardium and infarcted myocardium: up-regulation of essential transcription factor for angiogenesis, ets. *Gene Ther.* 7, 417–427.
- Apte, R.S., Barreiro, R.A., Duh, E., Volpert, O., Ferguson, T.A., 2004. Stimulation of neovascularization by the anti-angiogenic factor PEDF. *Invest. Ophthalmol. Vis. Sci.* 45, 4491–4497.
- Asahara, T., Takahashi, T., Masuda, H., Kalka, C., Chen, D., Iwaguro, H., Inai, Y., Silver, M., Isner, J.M., 1999. VEGF contributes to postnatal neovascularization by mobilizing bone marrow-derived endothelial progenitor cells. *EMBO J.* 18, 3964–3972.
- Bhargava, M., Joseph, A., Knesel, J., Halaban, R., Ki, Y., Pang, S., Goldberg, I., Setter, E., Donovan, M.A., Zarnegar, R., Michalopoulos, G.A., Nakamura, T., Faletto, D., Rosen, E.M., 1992. Scatter factor and hepatocyte growth factor: activities, properties, and mechanism. *Cell Growth Differ.* 3, 11–20.
- Birchmeier, C., Meyer, D., Riethmacher, D., 1995. Factors controlling growth, motility, and morphogenesis of normal and malignant epithelial cells. *Int. Rev. Cytol.* 160, 21–266.
- Bora, N.S., Kaliappan, S., Jha, P., Xu, Q., Sohn, J.H., Dhulakhandi, D.B., Kaplan, H.J., Bora, P.S., 2006. Complement activation via alternative pathway is critical in the development of laser-induced choroidal neovascularization: role of factor B and factor H. *J. Immunol.* 177, 1872–1878.
- Bora, P.S., Sohn, J.H., Cruz, J.M., Jha, P., Nishihori, H., Wang, Y., Kaliappan, S., Kaplan, H.J., Bora, N.S., 2005. Role of complement and complement membrane attack complex in laser-induced choroidal neovascularization. *J. Immunol.* 174, 491–497.
- Bottero, D.P., Rubin, J.S., Faletto, D.L., Chan, A.M., Kmiecik, T.E., Vande Woude, G.F., Aaronson, S.A., 1991. Identification of the hepatocyte growth factor receptor as the c-met proto-oncogene product. *Science* 251, 802–804.
- Bussolino, F., Di Renzo, M.F., Ziche, M., Bocchietto, E., Olivero, M., Naldini, L., Gaudino, G., Tamagnone, L., Coffa, A., Comoglio, P.M., 1992. Hepatocyte growth factor is a potent angiogenic factor which stimulates endothelial cell motility and growth. *J. Cell Biol.* 119, 629–641.
- Cai, J., Jiang, W.G., Ahmed, A., Boulton, M., 2006. Vascular endothelial growth factor-induced endothelial cell proliferation is regulated by interaction between VEGFR-2, SH-PTP1 and eNOS. *Microvasc. Res.* 71, 20–31.
- Cai, W., Rook, S.L., Jiang, Z.Y., Takahara, N., Aiello, L.P., 2000. Mechanisms of hepatocyte growth factor-induced retinal endothelial cell migration and growth. *Invest. Ophthalmol. Vis. Sci.* 41, 1885–1893.
- Caicedo, A., Espinosa-Heidmann, D.G., Piña, Y., Hernandez, E.P., Cousins, S.W., 2005. Blood-derived macrophages infiltrate the retina and activate Muller glial cells under experimental choroidal neovascularization. *Exp. Eye Res.* 81, 38–47.
- Campochiaro, P.A., 2000. Retinal and choroidal neovascularization. *J. Cell Physiol.* 184, 301–310.
- Campochiaro, P.A., 2006. Ocular versus extraocular neovascularization: mirror images or vague resemblances. *Invest. Ophthalmol. Vis. Sci.* 47, 462–474.
- Chan-Ling, T., Baxter, L., Afzal, A., Sengupta, N., Caballero, S., Rosinova, E., Grant, M.B., 2006. Hematopoietic stem cells provide repair functions after laser-induced Bruch's membrane rupture model of choroidal neovascularization. *Am. J. Pathol.* 168, 1031–1044.
- Claus, P., Doring, F., Gringel, S., Müller-Ostermeyer, F., Fuhrrott, J., Kraft, T., Grothe, C., 2003. Differential intranuclear localization of fibroblast growth factor-2 isoforms and specific interaction with the survival of motoneuron protein. *J. Biol. Chem.* 278, 479–485.
- Csaky, K.G., Baffi, J.Z., Byrnes, G.A., Wolfe, J.D., Hilmer, S.C., Flippin, J., Cousins, S.W., 2004. Recruitment of marrow-derived endothelial cells to experimental choroidal neovascularization by local expression of vascular endothelial growth factor. *Exp. Eye Res.* 78, 1107–1116.
- Edelman, J.L., Castro, M.R., 2000. Quantitative image analysis of laser-induced choroidal neovascularization in rat. *Exp. Eye Res.* 71, 523–533.
- Eichler, W., Yafai, Y., Wiedemann, P., Fengler, D., 2006. Antineovascular agents in the treatment of eye diseases. *Curr. Pharm. Des.* 12, 2645–2660.
- Espinosa-Heidmann, D.G., Caicedo, A., Hernandez, E.P., Csaky, K.G., Cousins, S.W., 2003. Bone marrow-derived progenitor cells contribute to experimental choroidal neovascularization. *Invest. Ophthalmol. Vis. Sci.* 44, 4914–4919.
- Espinosa-Heidmann, D.G., Reinoso, M.A., Pina, Y., Csaky, K.G., Caicedo, A., Cousins, S.W., 2005. Quantitative enumeration of vascular smooth muscle cells and endothelial cells derived from bone marrow precursors in experimental choroidal neovascularization. *Exp. Eye Res.* 80, 369–378.
- Frank, R.N., 1997. Growth factors in age-related macular degeneration: pathogenic and therapeutic implications. *Ophthalmic Res.* 29, 341–353.
- Frank, R.N., Amin, R.H., Elliott, D., Puklin, J.E., Abrams, G.W., 1996. Basic fibroblast growth factor and vascular endothelial growth factor are present in epiretinal and choroidal neovascular membranes. *Am. J. Ophthalmol.* 122, 393–403.
- Garcia, M., Vecino, E., 2003. Role of Müller glia in neuroprotection and regeneration in the retina. *Histol Histopathol* 18, 1205–1218.
- Geisen, P., McColm, J.R., Hartnett, M.E., 2006. Choroidal endothelial cells transigrate across the retinal pigment epithelium but do not proliferate in response to soluble vascular endothelial growth factor. *Exp. Eye Res.* 82, 608–619.
- Gerritsen, M.E., 2005. HGF and VEGF: a dynamic duo. *Circ Res.* 96, 272–273.
- Gerritsen, M.E., Tomlinson, J.E., Zlot, C., Ziman, M., Hwang, S., 2003. Using gene expression profiling to identify the molecular basis of the synergistic actions of hepatocyte growth factor and vascular endothelial growth factor in human endothelial cells. *Br. J. Pharmacol.* 140, 595–610.
- Gille, J., Khalik, M., König, V., Kaufmann, R., 1998. Hepatocyte growth factor/scatter factor (HGF/SF) induces vascular permeability factor (VPF/VEGF) expression by cultured keratinocytes. *J. Invest. Dermatol.* 111, 1160–1165.
- Grant, D.S., Kleinman, H.K., Goldberg, I.D., Bhargava, M.M., Nickoloff, B.J., Kinsella, J.L., Polverini, P., Rosen, E.M., 1993. Scatter factor induces blood vessel formation in vivo. *Proc. Natl. Acad. Sci. USA* 90, 1937–1941.
- Grierson, I., Heathcote, L., Hiscott, P., Hogg, P., Briggs, M., Hagan, S., 2000. Hepatocyte growth factor/scatter factor in the eye. *Prog. Retin. Eye Res.* 19, 779–802.
- Hayashi, A., Kim, H.C., de Juan Jr, E., 1999. Alterations in protein tyrosine kinase pathways following retinal vein occlusion in the rat. *Curr. Eye Res.* 18, 231–239.
- He, P.M., He, S., Garner, J.A., Ryan, S.J., Hinton, D.R., 1998. Retinal pigment epithelial cells secrete and respond to hepatocyte growth factor. *Biochem. Biophys. Res. Commun.* 249, 253–257.
- Hoffmann, S., He, S., Ehren, M., Ryan, S.J., Wiedemann, P., Hinton, D.R., 2006. MMP-2 and MMP-9 secretion by RPE is stimulated by angiogenic molecules found in choroidal neovascular membranes. *Retina* 26, 454–461.
- Hollborn, M., Jahn, K., Limb, G.A., Kohen, L., Wiedemann, P., Bringmann, A., 2004. Characterization of the basic fibroblast growth factor-evoked proliferation of the human Müller cell line, MIO-M1. *Graefes Arch. Clin. Exp. Ophthalmol.* 42, 414–422.
- Hu, W., Criswell, M.H., Ottlecz, A., Cornell, T.L., Danis, R.P., Lambrou, G.N., Ciulla, T.A., 2005. Oral administration of lumiracoxib reduces choroidal neovascular membrane development in the rat laser-trauma model. *Retina* 25, 1054–1064.
- Imanishi, T., Hano, T., Matsuo, Y., Nishio, I., 2003. Oxidized low-density lipoprotein inhibits vascular endothelial growth factor-induced endothelial progenitor cell differentiation. *Clin. Exp. Pharmacol. Physiol.* 30, 665–670.
- Ishida, K., Yoshimura, N., Mandai, M., Honda, Y., 1999. Inhibitory effect of TNF-470 on experimental choroidal neovascularization in a rat model. *Invest. Ophthalmol. Vis. Sci.* 40, 1512–1519.
- Issbrücker, K., Marti, H.H., Hippenstiel, S., Springmann, G., Voswinkel, R., Gaumann, A., Breier, G., Drexler, H.C., Suttrop, N., Claus, M., 2003. p38 MAP kinase – a molecular switch between VEGF-induced angiogenesis and vascular hyperpermeability. *FASEB J.* 17, 262–264.
- Klagsbrun, M., Smith, S., Sullivan, R., Shing, Y., Davidson, S., Smith, J.A., Sasse, J., 1987. Multiple forms of basic fibroblast growth factor: amino-terminal cleavages by tumor cell- and brain cell-derived acid proteinases. *Proc. Natl. Acad. Sci. USA* 84, 1839–1843.
- Koochekpour, S., Jeffers, M., Rulong, S., Taylor, G., Klineberg, E., Hudson, E.A., Resau, J.H., Vande Woude, G.F., 1997. Met and hepatocyte growth factor/scatter factor expression in human gliomas. *Cancer Res.* 57, 5391–5398.
- Krasnici, S., Werner, A., Eichhorn, M.E., Schmitt-Sody, M., Pahernik, S.A., Sauer, B., Schulze, B., Teifel, M., Michaelis, U., Naujoks, K., Dellian, M., 2003. Effect of the surface charge of liposomes on their uptake by angiogenic tumor vessels. *Int. J. Cancer* 105, 561–567.
- Kuhlmann, C.R., Schaefer, C.A., Fehsecke, A., Most, A.K., Tillmanns, H., Erdogan, A., 2005. A new signaling mechanism of hepatocyte growth factor-induced endothelial proliferation. *J. Thromb. Haemost.* 3, 2089–2095.
- Kvanta, A., Alvgren, P.V., Berglin, L., Seregard, S., 1996. Subfoveal fibrovascular membranes in age-related macular degeneration express vascular endothelial growth factor. *Invest. Ophthalmol. Vis. Sci.* 37, 1929–1934.
- Kwak, N., Okamoto, N., Wood, J.M., Campochiaro, P.A., 2000. VEGF is major stimulator in model of choroidal neovascularization. *Invest. Ophthalmol. Vis. Sci.* 41, 3158–3164.
- Lashkari, K., Rahimi, N., Kazlauskas, A., 1999. Hepatocyte growth factor receptor in human RPE cells: implications in proliferative vitreoretinopathy. *Invest. Ophthalmol. Vis. Sci.* 40, 149–156.
- Liou, G.I., Matragoon, S., Samuel, S., Behzadian, M.A., Tsai, N.T., Gu, X., Roon, P., Hunt, R.C., Caldwell, R.B., Marcus, D.M., 2002. MAP kinase and β -catenin signaling in HGF induced RPE migration. *Mol. Vis.* 8, 483–493.
- Lip, P.L., Blann, A.D., Hope-Ross, M., Gibson, J.M., Lip, G.Y., 2001. Age-related macular degeneration is associated with increased vascular endothelial growth factor, hemorheology and endothelial dysfunction. *Ophthalmology* 108, 705–710.
- Martin, G., Schlunck, G., Hansen, L.L., Agostini, H.T., 2004. Differential expression of angioregulatory factors in normal and CNV-derived human retinal pigment epithelium. *Graefes Arch. Clin. Exp. Ophthalmol.* 42, 321–326.
- Martin, T.A., Mansel, R., Jiang, W.G., 2001. Hepatocyte growth factor modulates vascular endothelial-cadherin expression in human endothelial cells. *Clin. Cancer Res.* 7, 734–737.
- Matsumoto, K., Nakamura, T., 1996. Emerging multipotent aspects of hepatocyte growth factor. *J. Biochem. (Tokyo)* 119, 591–600.
- Matsumoto, M., Ogata, N., Takada, Y., Tobe, T., Yamada, H., Takahashi, K., Uyama, M., 1996. FGF receptor 1 expression in experimental choroidal neovascularization. *Jpn. J. Ophthalmol.* 40, 329–338.
- Miyashiro, M., Ogata, N., Takahashi, K., Matsumoto, M., Yamamoto, C., Yamada, H., Uyama, M., 1998. Expression of basic fibroblast growth factor and its receptor

- mRNA in retinal tissue following ischemic injury in the rat. *Graefes Arch. Clin. Exp. Ophthalmol.* 236, 295–300.
- Montesano, R., Matsumoto, K., Nakamura, T., Orci, L., 1991. Identification of a fibroblast-derived epithelial morphogen as hepatocyte growth factor. *Cell* 67, 901–908.
- Müller-Ostermeyer, F., Claus, P., Grothe, C., 2001. Distinctive effects of rat fibroblast growth factor-2 isoforms on PC12 and Schwann cells. *Growth Factors* 19, 175–191.
- Murayama, T., Asahara, T., 2002. Bone marrow-derived endothelial progenitor cells for vascular regeneration. *Curr. Opin. Mol. Ther.* 4, 395–402.
- Nagineni, C.N., Samuel, W., Nagineni, S., Pardhasaradhi, K., Wiggert, B., Detrick, B., Hooks, J.J., 2003. Transforming growth factor- β induces expression of vascular endothelial growth factor in human retinal pigment epithelial cells: involvement of mitogen-activated protein kinases. *J. Cell Physiol.* 197, 453–462.
- Nakamura, Y., Morishita, R., Higaki, J., Kida, I., Aoki, M., Moriguchi, A., Yamada, K., Hayashi, S.I., Yo, Y., Matsumoto, K., Nakamura, T., Ogihara, T., 1995. Expression of local hepatocyte growth factor system in vascular tissues. *Biochem. Biophys. Res. Commun.* 215, 483–488.
- Nakamura, Y., Morishita, R., Higaki, J., Kida, I., Aoki, M., Moriguchi, A., Yamada, K., Hayashi, S., Yo, Y., Nakano, H., Matsumoto, K., Nakanura, T., Ogihara, T., 1996. Hepatocyte growth factor is a novel member of the endothelium-specific growth factors: additive stimulatory effect of hepatocyte growth factor with basic fibroblast growth factor but not with vascular endothelial growth factor. *J. Hypertens.* 14, 1067–1072.
- Ogata, N., Matsushima, M., Takada, Y., Tobe, T., Takahashi, K., Yi, X., Yamamoto, C., Yamada, H., Uyama, M., 1996. Expression of basic fibroblast growth factor mRNA in developing choroidal neovascularization. *Curr. Eye Res.* 15, 1008–1018.
- Ogata, N., Yamanaka, R., Yamamoto, C., Miyashiro, M., Kimoto, T., Takahashi, K., Maruyama, K., Uyama, M., 1998. Expression of vascular endothelial growth factor and its receptor, KDR, following retinal ischemia-reperfusion injury in the rat. *Curr. Eye Res.* 17, 1087–1096.
- Ohsato, M., Hayashi, H., Oshima, K., Koji, T., Nakane, P., 1997. In situ localization of basic fibroblast growth factor protein and mRNA in the retina. *Ophthalmic Res.* 29, 24–30.
- Papetti, M., Shujath, J., Riley, K.N., Herman, I.M., 2003. FGF-2 antagonizes the TGF- β 1-mediated induction of pericyte α -smooth muscle actin expression: a role for myf-5 and Smad-mediated signaling pathways. *Invest. Ophthalmol. Vis. Sci.* 44, 4994–5005.
- Powell, P.P., Klagsbrun, M., 1991. Three forms of rat basic fibroblast growth factor are made from a single mRNA and localize to the nucleus. *J. Cell Physiol.* 148, 202–210.
- Rajashekhar, G., Traktuev, D.O., Roell, C.W., Johnstone, B.H., Merfeld-Claus, S., Van Natta, B., Rosen, E.D., March, K.L., Claus, M., 2008. IFATS collection: adipose stromal cell differentiation is reduced by endothelial cell contact and paracrine communication: role of canonical Wnt-signaling. *Stem Cells* 26, 2674–2681.
- Reisinger, K., Kaufmann, R., Gille, J., 2003. Increased Sp1 phosphorylation as a mechanism of hepatocyte growth factor (HGF/SF)-induced vascular endothelial growth factor (VEGF/VPF) transcription. *J. Cell Sci.* 116, 225–238.
- Rosen, E.M., Grant, D., Kleinman, H., Jaken, S., Donovan, M.A., Setter, E., Luckett, P.M., Carley, W., Bhargava, M., Goldberg, I.D., 1991. Scatter factor stimulates migration of vascular endothelium and capillary-like tube formation. *EXS* 59, 76–88.
- Rosen, E.M., Grant, D.S., Kleinman, H.K., Goldberg, I.D., Bhargava, M.M., Nickoloff, B.J., Kinsella, J.L., Polverini, P., 1993a. Scatter factor (hepatocyte growth factor) is a potent angiogenesis factor in vivo. *Symp. Soc. Exp. Biol.* 47, 227–234.
- Rosen, E.M., Zitnik, R.J., Elias, J.A., Bhargava, M.M., Wines, J., Goldberg, I.D., 1993b. The interaction of HGF-SF with other cytokines in tumor invasion and angiogenesis. *EXS* 65, 301–310.
- Rosenthal, R., Malek, G., Salomon, N., Peill-Meininghaus, M., Coepicus, L., Wohlleben, H., Wimmers, S., Bowes Rickman, C., Strauss, O., 2005. The fibroblast growth factor receptors, FGFR-1 and FGFR-2, mediate two independent signalling pathways in human retinal pigment epithelial cells. *Biochem. Biophys. Res. Commun.* 337, 241–247.
- Rousseau, B., Larrieu-Lahargue, F., Bikfalvi, A., Javerzat, S., 2003. Involvement of fibroblast growth factors in choroidal angiogenesis and retinal vascularization. *Exp. Eye Res.* 77, 147–156.
- Rubin, J.S., Bottaro, D.P., Aaronson, S.A., 1993. Hepatocyte growth factor/scatter factor and its receptor, the c-met proto-oncogene product. *Biochim. Biophys. Acta* 1155, 357–371.
- Schmidt, N.O., Westphal, M., Hagel, C., Ergün, S., Stavrou, D., Rosen, E.M., Lamszus, K., 1999. Levels of vascular endothelial growth factor, hepatocyte growth factor/scatter factor and basic fibroblast growth factor in human gliomas and their relation to angiogenesis. *Int. J. Cancer* 84, 10–18.
- Schweigerer, L., Mallerstein, B., Neufeld, G., Gospodarowicz, D., 1987. Basic fibroblast growth factor is synthesized in cultured retinal pigment epithelial cells. *Biochem. Biophys. Res. Commun.* 143, 934–940.
- Seghezzi, G., Patel, S., Ren, C.J., Gualandris, A., Pintucci, G., Robbins, E.S., Shapiro, R.L., Galloway, A.C., Rifkin, D.B., Mignatti, P., 1998. Fibroblast growth factor-2 (FGF-2) induces vascular endothelial growth factor (VEGF) expression in the endothelial cells of forming capillaries: an autocrine mechanism contributing to angiogenesis. *J. Cell Biol.* 141, 1659–1673.
- Sengupta, N., Caballero, S., Mames, R.N., Butler, J.M., Scott, E.W., Grant, M.B., 2003. The role of adult bone marrow-derived stem cells in choroidal neovascularization. *Invest. Ophthalmol. Vis. Sci.* 44, 4908–4913.
- Sengupta, S., Gherardi, E., Sellers, L.A., Wood, J.M., Sasisekharan, R., Fan, T.P., 2003. Hepatocyte growth factor/scatter factor can induce angiogenesis independently of vascular endothelial growth factor. *Arterioscler. Thromb. Vasc. Biol.* 23, 69–75.
- Shen, W.Y., Yu, M.J., Barry, C.J., Constable, I.J., Rakoczy, P.E., 1998. Expression of cell adhesion molecules and vascular endothelial growth factor in experimental choroidal neovascularisation in the rat. *Br. J. Ophthalmol.* 82, 1063–1071.
- Sheridan, C.M., Rice, D., Hiscott, P.S., Wong, D., Kent, D.L., 2006. The presence of AC133-positive cells suggests a possible role of endothelial progenitor cells in the formation of choroidal neovascularization. *Invest. Ophthalmol. Vis. Sci.* 47, 1642–1645.
- Shibuki, H., Katai, N., Kuroiwa, S., Kurokawa, T., Arai, J., Matsumoto, K., Nakamura, T., Yoshimura, N., 2002. Expression and neuroprotective effect of hepatocyte growth factor in retinal ischemia-reperfusion injury. *Invest. Ophthalmol. Vis. Sci.* 43, 528–536.
- Silvagno, F., Follenzi, A., Arese, M., Prat, M., Giraudo, E., Gaudino, G., Camussi, G., Comoglio, P.M., Bussolino, F., 1995. In vivo activation of met tyrosine kinase by heterodimeric hepatocyte growth factor molecule promotes angiogenesis. *Arterioscler. Thromb. Vasc. Biol.* 15, 1857–1865.
- Spilsbury, K., Garrett, K.L., Shen, W.Y., Constable, I.J., Rakoczy, P.E., 2000. Overexpression of vascular endothelial growth factor (VEGF) in the retinal pigment epithelium leads to the development of choroidal neovascularization. *Am. J. Pathol.* 157, 135–144.
- Taniyama, Y., Morishita, R., Aoki, M., Nakagami, H., Yamamoto, K., Yamazaki, K., Matsumoto, K., Nakamura, T., Kaneda, Y., Ogihara, T., 2001a. Therapeutic angiogenesis induced by human hepatocyte growth factor gene in rat and rabbit hindlimb ischemia models: preclinical study for treatment of peripheral arterial disease. *Gene Ther.* 8, 181–189.
- Taniyama, Y., Morishita, R., Hiraoka, K., Aoki, M., Nakagami, H., Yamasaki, Y., Matsumoto, K., Nakamura, T., Kaneda, Y., Ogihara, T., 2001b. Therapeutic angiogenesis induced by human hepatocyte growth factor gene in rat diabetic hind limb ischemia model: molecular mechanisms of delayed angiogenesis in diabetes. *Circulation* 104, 2344–2350.
- Tobe, T., Ortega, S., Luna, J.D., Ozaki, H., Okamoto, N., Derevjani, N.L., Vinore, S.A., Basilio, C., Campochiaro, P.A., 1998. Targeted disruption of the FGF2 gene does not prevent choroidal neovascularization in a murine model. *Am. J. Pathol.* 153, 1641–1646.
- Tsarfaty, I., Resau, J.H., Rulong, S., Keydar, I., Faletto, D.L., Vande Woude, G.F., 1992. The met proto-oncogene receptor and lumen formation. *Science* 257, 1258–1261.
- Tsarfaty, I., Rong, S., Resau, J.H., Rulong, S., da Silva, P.P., Vande Woude, G.F., 1994. The met proto-oncogene mesenchymal to epithelial cell conversion. *Science* 263, 98–101.
- Van Belle, E., Witzensbichler, B., Chen, D., Silver, M., Chang, L., Schwall, R., Isner, J.M., 1998. Potentiated angiogenic effect of scatter factor/hepatocyte growth factor via induction of vascular endothelial growth factor: the case for paracrine amplification of angiogenesis. *Circulation* 97, 381–390.
- Vlodavsky, I., Folkman, J., Sullivan, R., Fridman, R., Ishai-Michaeli, R., Sasse, J., Klagsbrun, M., 1987. Endothelial cell-derived basic fibroblast growth factor: synthesis and deposition into subendothelial extracellular matrix. *Proc. Natl. Acad. Sci. USA* 84, 2292–2296.
- Wada, M., Ogata, N., Otsuji, T., Uyama, M., 1999. Expression of vascular endothelial growth factor and its receptor (KDR/flk-1) mRNA in experimental choroidal neovascularization. *Curr. Eye Res.* 18, 203–213.
- Wang, F., Rendahl, K.G., Manning, W.C., Quiroz, D., Coyne, M., Miller, S.S., 2003. AAV-mediated expression of vascular endothelial growth factor induces choroidal neovascularization in rat. *Invest. Ophthalmol. Vis. Sci.* 44, 781–790.
- Wang, Y.S., Eichler, W., Friedrichs, U., Yafai, Y., Hoffmann, S., Yasukawa, T., Hui, Y.N., Wiedemann, P., 2005. Impact of endostatin on bFGF-induced proliferation, migration, and matrix metalloproteinase-2 expression/secretion of bovine choroidal endothelial cells. *Curr. Eye Res.* 30, 479–489.
- Wojta, J., Kaun, C., Breuss, J.M., Koshelnick, Y., Beckmann, R., Hattey, E., Mildner, M., Weninger, W., Nakamura, T., Tschachler, E., Binder, B.R., 1999. Hepatocyte growth factor increases expression of vascular endothelial growth factor and plasminogen activator inhibitor-1 in human keratinocytes and the vascular endothelial growth factor receptor flk-1 in human endothelial cells. *Lab. Invest.* 79, 427–438.
- Xia, P., Aiello, L.P., Ishii, H., Jiang, Z.Y., Park, D.J., Robinson, G.S., Takagi, H., Newsome, W.P., Jirousek, M.R., King, G.L., 1996. Characterization of vascular endothelial growth factor's effect on the activation of protein kinase C, its isoforms, and endothelial cell growth. *J. Clin. Invest.* 98, 2018–2026.
- Xin, X., Yang, S., Ingle, G., Zlot, C., Rangell, L., Kowalski, J., Schwall, R., Ferrara, N., Gerritsen, M.E., 2001. Hepatocyte growth factor enhances vascular endothelial growth factor-induced angiogenesis in vitro and in vivo. *Am. J. Pathol.* 158, 1111–1120.
- Yamamoto, C., Ogata, N., Matsushima, M., Takahashi, K., Miyashiro, M., Yamada, H., Maeda, H., Uyama, M., Matsuzaki, K., 1996a. Gene expressions of basic fibroblast growth factor and its receptor in healing of rat retina after laser photocoagulation. *Jpn. J. Ophthalmol.* 40, 480–490.
- Yamamoto, C., Ogata, N., Yi, X., Takahashi, K., Miyashiro, M., Yamada, H., Uyama, M., Matsuzaki, K., 1996b. Immunolocalization of basic fibroblast growth factor during wound repair in rat retina after laser photocoagulation. *Graefes Arch. Clin. Exp. Ophthalmol.* 234, 695–702.
- Yi, X., Ogata, N., Komada, M., Yamamoto, C., Takahashi, K., Omori, K., Uyama, M., 1997. Vascular endothelial growth factor expression in choroidal neovascularization in rats. *Graefes Arch. Clin. Exp. Ophthalmol.* 235, 313–319.
- Zubilewicz, A., Hecquet, C., Jeanny, J.C., Soubraane, G., Courtois, Y., Mascarelli, F., 2001. Two distinct signalling pathways are involved in FGF2-stimulated proliferation of choriocapillary endothelial cells: a comparative study with VEGF. *Oncogene* 20, 1403–1413.